Supplementary Information

pH-Dependent Inversion of Optical Activity in Chiral Mesostructured In_2S_3 Induced by Cysteine

Methods

Synthesis of CMI, RMI and AMI

All samples were synthesized *via* a hydrothermal method.[1] In a typical synthesis, varying volumes of 1 M NaOH were added to the beakers. Ultrapure water was added to each beaker to ensure the total volumes of the solutions remained constant. Next, 10 mL of 0.4 M cysteine (4.0 mmol) was added to the beakers, and the mixture was magnetically stirred at 500 rpm for 20 min to prepare solution A. Subsequently, 10 mL of 0.1 M $InCl_3 \cdot 4H_2O$ (1.0 mmol) was introduced into solution A and stirred at 500 rpm for another 20 min to generate the precursor solution. The pH value of the precursor solution was measured by a SMART SENSOR pen-type pH meter. Thereafter, 30 mL of the precursor solution was transferred into a 50 mL Teflon-lined stainless-steel autoclave. Finally, the autoclave was sealed, heated to 150 ℃, and maintained at this temperature for 10 h. After cooling to room temperature, the precipitates were collected by centrifugation, washed several times with ultrapure water and ethanol, and lyophilized or dried in a vacuum oven at 50 ℃. The syntheses of RMI and AMI followed a similar protocol, but used racemic Cys (0.484 g, 4.0 mmol) and thioacetamide (TAA, 0.30 g, 4.0 mmol) as the sulfur sources instead of L/D-Cys, respectively.

FTIR

FTIR spectra of powder samples were collected with a PerkinElmer FTIR spectrometer.

XRD

The crystal structures of CMI, RMI and AMI were examined by powder XRD, which was collected on a Rigaku MiniFlex 600 X-ray diffractometer equipped with Cu Kα (λ = 1.5418 Å) radiation working at an acceleration voltage of 40 kV and a current of 15 mA. The scanning rate was set to 0.06° s^{-1}.

SEM

Low-magnification SEM images were obtained using a JEOL JSM-7800 with an accelerating voltage of 5.0 kV.

DRUV–vis and DRCD

Diffuse reflection UV–vis spectrum (DRUV–vis) and diffuse reflection circular dichroism (DRCD) spectra were obtained on a JASCO J-1500 spectropolarimeter fitted with a DRCD apparatus using powder samples (Fig. S1), and data were collected with a scanning rate of 500 nm min^{-1} ranging from 200 to 700 nm at 293 K. The incident light used in the instrument is circularly polarized light. Baseline corrections were performed using the pure $BaSO_4$ matrix. Artefacts, such as the linear dichroism of all CD spectra, were eliminated by the accumulation of data generated at eight rotation degrees in the range of 360°.

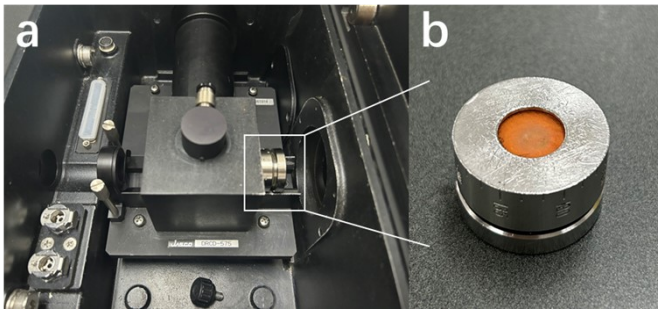

Fig. S1 Pictures of details in DRCD measurement. **a,** DRCD apparatus and sample placement area. **b,** Prepared sample for DRCD. The scale on the sample stage can be utilized for alignment and positioning during multi-angle measurements.

Materials

Indium chloride tetrahydrate ($InCl_3 \cdot 4H_2O$) (99.0%), L-cysteine (L-Cys) (99.0%), Thioacetamide (TAA) (99.0%) and racemic cysteine (rac-Cys) (99.0%) were purchased from Adamas Ltd. D-Cys (98%) was purchased from Shanghai Aladdin Biochemical Technology Co., Ltd. Sodium hydroxide (99.9%) were purchased from Shanghai Macklin Biochemical Co., Ltd. All chemicals and solvents were used without further purification.

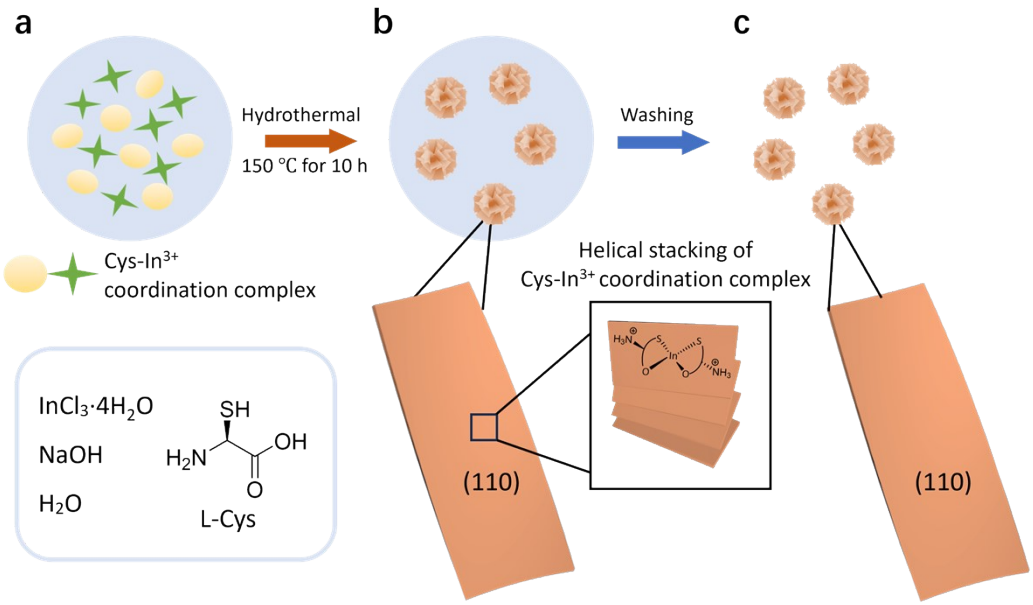

Fig. S2 Schematic illustration for the synthesis process of CMI. **a,** Formation of In^{3+} and S^{2-} complexes in a mixture of $InCl_3 \cdot 4H_2O$, L-Cys, NaOH and deionized water. **b,** Growth of CMI during a hydrothermal process at 150 °C for 10 h. Chirality transfer from chiral organic molecule to as-made L-CMI. **c,** L-CMI without organics (L-Cys) can be obtained by washing.

L/D-Cys serves as both the sulfur source and the symmetry-breaking agent (Fig. S2a). The formation process is initiated by the coordination between L/D-Cys and In^{3+}, forming an L/D-Cys-In^{3+} complex that subsequently decomposes under hydrothermal conditions to yield In_2S_3 nuclei. Driven by the structure-directing effect of L/D-Cys, the In_2S_3 seeds develop into helical nanoflakes, which then self-assemble into nanoflower architectures. The selective adsorption of Cys onto the (110) facets restricts random agglomeration and dictates crystal growth along the [110] zone axis. The chirality of the resulting In_2S_3 nanoflakes originates from the asymmetric bonding environment (In-S and In-COO) around the Cys stereocenter, which steers the dislocation-driven growth of the nanocrystals. During the subsequent ripening stage, oriented attachment further drives the helical nanoflakes to construct hierarchical nanoflower morphologies. Finally, after removing Cys through the washing step, organic-free L/D-CMI can be obtained (Fig. S2c).

Table S1 Experimental conditions.

Sample No.	L-, D-, rac-Cys, TAA /mmol	$InCl_3 \cdot 4H_2O$ /mmol	NaOH /mmol	V_{total} /mL	Temp. /°C	Time /h	pH
1	4.0	1.0	3.2	30.0	150	10	4.53
2			3.6				5.50
3			4.0				6.20
4			4.4				6.93
5			4.8				7.60
6			5.2				8.04
7			5.6				8.35
8			6.0				8.60
9			6.4				9.12

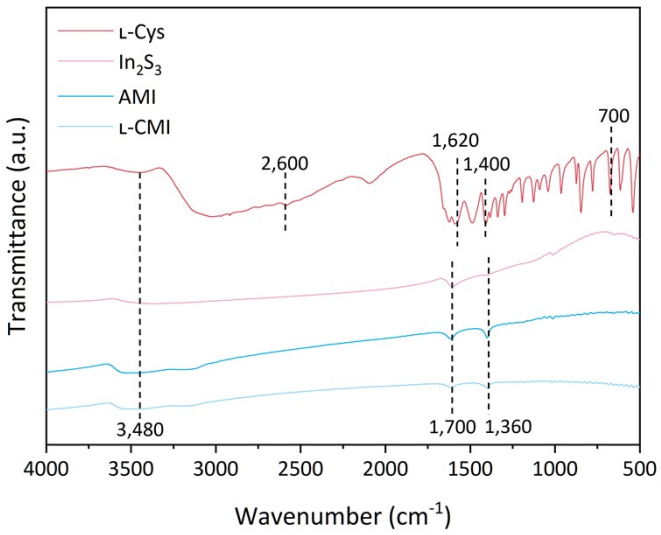

Fig. S3 FTIR spectra of L-Cys, commercially bought In_2S_3, AMI and L-CMI.

The FTIR spectra of L-Cys, commercial In_2S_3, AMI, and L-CMI were measured (Fig. S3). For pure L-Cys, the absorption bands near 700 and 1,400 cm^{-1} are attributed to C-S stretching and symmetric -COO^- stretching vibrations, respectively.[2] The absence of these Cys-related peaks in the spectra of both L-CMI and commercial In_2S_3 confirms the complete elimination of L-Cys after washing. Furthermore, L-CMI, AMI, and commercial In_2S_3 show highly comparable spectra. The absorption at 1,360 cm^{-1} is assigned to S-O vibrations caused by surface oxidation of In_2S_3 in air, distinct from the 1,400 cm^{-1} carboxylate signal of L-Cys. The 1,700 cm^{-1} peak is attributed to In-S bonds.[3] A broad band near 3,480 cm^{-1} and a peak at 1,620 cm^{-1} correspond to the stretching and bending vibrations of surface-adsorbed and structural water molecules, respectively.

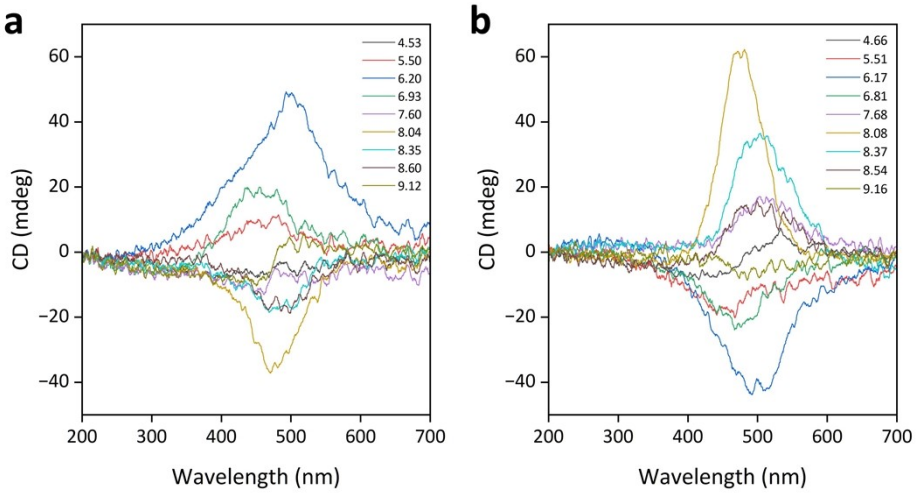

Fig. S4 CD spectra with intensity of **a,** L1-L9; **b,** D1-D9.

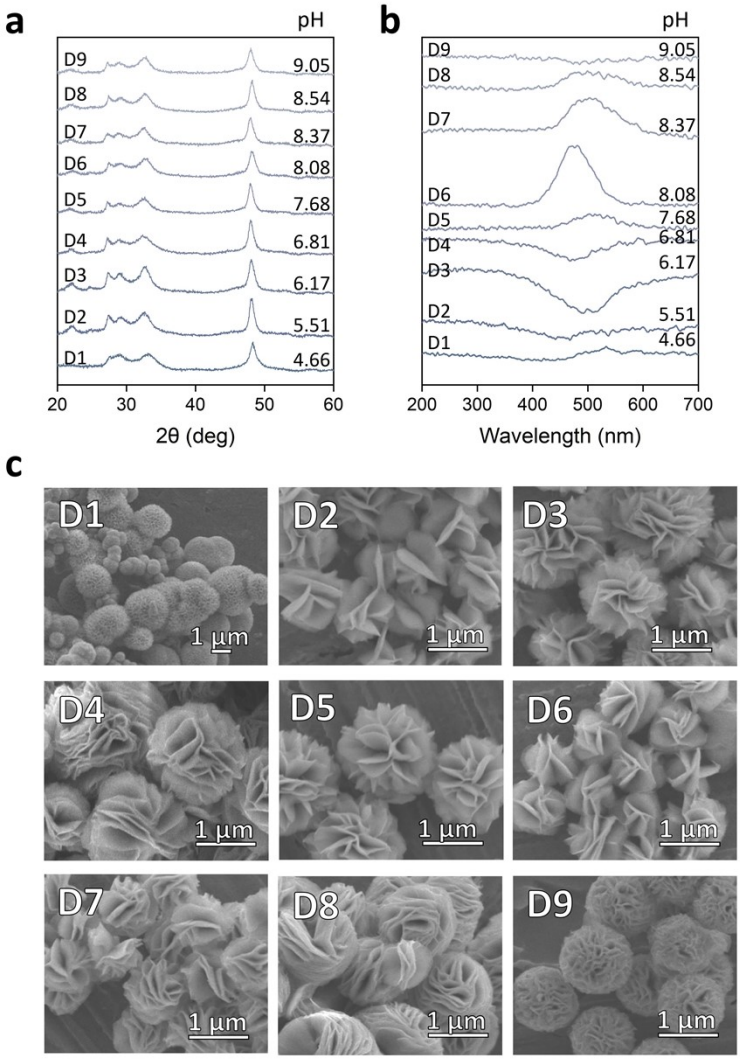

Fig. S5 Characterizations of D-CMIs synthesized at different alkaline conditions. **a,** XRD patterns. **b,** DRCD spectra. **c,** SEM images.

All samples are identified as a cubic phase of In_2S_3 (β-In_2S_3, JCPDS Card No. 32-

0456) with the space group of $Fd\bar{3}m$ and unit cell parameter a of 10.82 Å. All XRD patterns exhibit characteristic diffraction peaks, with strong signals at 2θ values of 27.3°, 28.8°, 32.4°, and 48.1°, corresponding to the 311, 222, 400, and 440 reflections, respectively, indicating the preferred crystallographic orientations of <110>.

During the inversion process, the CD signals exhibit a distinct trend of initial attenuation followed by subsequent enhancement (Fig. 2 and Fig. S5). This phenomenon indicates a competitive cancellation effect between the opposing CD signals driven by different underlying mechanisms.

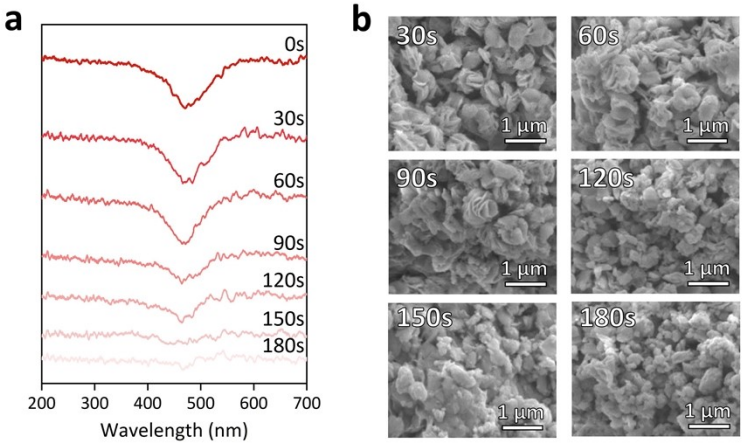

Fig. S6 a, DRCD of L5 with various grinding time. **b,** corresponding SEM images of L5 with various grinding time.

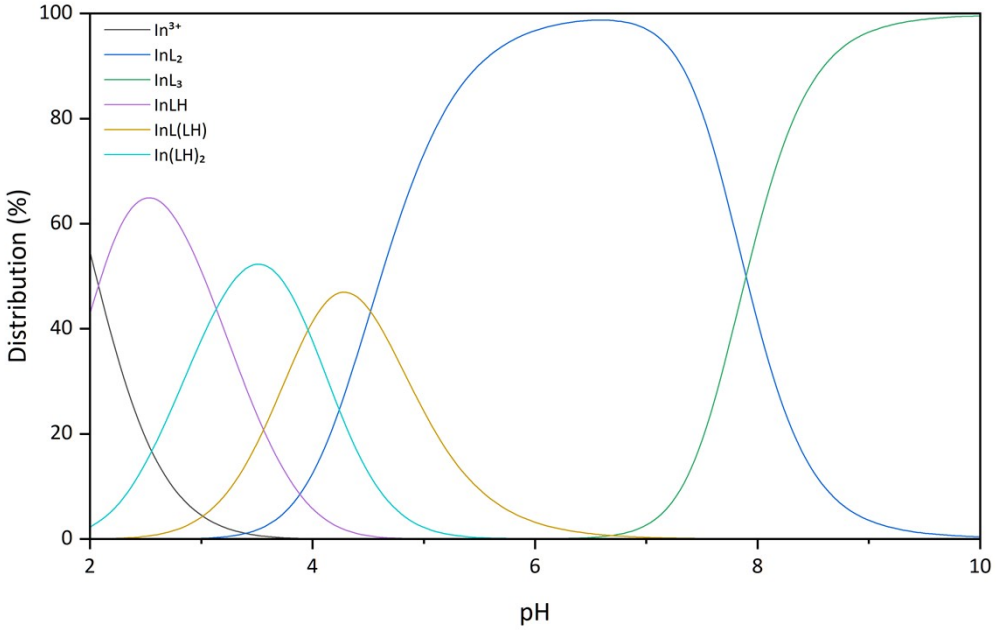

Fig. S7 The pH-dependent distribution diagram of the coordination species, calculated using the stability constants.[4]

Table S2 pH values of multiple groups of L-CMI samples. The measurement error of the pH value is within ±0.05.

	L1	L2	L3	L4	L5	L6	L7	L8	L9
pH-1	4.28	5.42	6.10	6.68	7.78	8.15	8.43	8.69	9.02
pH-2	4.46	5.56	6.34	7.04	7.41	8.03	8.31	8.56	9.12
pH-3	4.86	5.52	6.16	7.06	7.62	7.93	8.32	8.55	9.22
average pH	4.53	5.50	6.20	6.93	7.60	8.04	8.35	8.60	9.12

Table S3 pH values of multiple groups of D-CMI samples. The measurement error of the pH value is within ±0.05.

	D1	D2	D3	D4	D5	D6	D7	D8	D9
pH	4.66	5.51	6.17	6.81	7.68	8.08	8.37	8.54	9.16

References

1. T. S. Metzger, H. Batchu, A. Kumar, D. A. Fedotov, N. Goren, D. K. Bhowmick, I. Shioukhi, S. Yochelis, I. Schapiro, R. Naaman, O. Gidron and Y. Paltiel, *Journal of the American Chemical Society*, 2023, **145**, 3972-3977.
2. W. Luo, A. Li, B. Yang, H. Pang, J. Fu, G. Chen, M. Liu, X. Liu, R. Ma, J. Ye and N. Zhang, *ACS Applied Materials & Interfaces*, 2023, **15**, 15387-15395.
3. H. Chen, S. Gao, G. Huang, Q. Chen, Y. Gao and J. Bi, *Applied Catalysis B: Environmental*, 2024, **343**, 123545.
4. N. Kojima, Y. Sugiura and H. Tanaka, *Bulletin of the Chemical Society of Japan*, 1976, **49**, 3023-3028.